



Cite this: *Chem. Commun.*, 2025, 61, 6599

Received 27th January 2025,
Accepted 3rd April 2025

DOI: 10.1039/d5cc00510h

rsc.li/chemcomm

Achieving extreme thermal stability of high-silica FAU through trace water-assisted steam treatment†

Boqing Li,^a Raquel Simancas,^{ib} Kenta Iyoki,^{abc} Shanmugam P. Elangovan,^d Takahiro Ohkubo,^{ib} Tatsuya Okubo^{ib} and Toru Wakihara^{ib}*^{ad}

This study explores defect-healing via heat/steam treatments to enhance FAU's thermal stability. The optimal steam treatment with 1% humidity retained 69% relative crystallinity after the heat resistance test at 1150 °C for 24 h, halving the crystallinity loss vs. the untreated sample. This approach provides zeolites with exceptional thermal stability.

Zeolites, crystalline aluminosilicate materials characterized by their porous structures, have been widely used in various industrial applications, including catalysis, adsorption, and ion exchange.^{1–3} However, their stability under extreme conditions, such as high temperatures (e.g., 1000 °C), remains a significant challenge, particularly for aluminosilicate zeolites.^{4,5} The degradation of high-silica zeolites under harsh conditions is often attributed to the presence of silanol groups within the zeolite framework, which can compromise thermal stability and diminish their overall performance.⁶ Addressing these limitations requires the development of effective post-synthetic defect-healing strategies that enhance the thermal stability and robustness of zeolites. Heat and steam treatments are the most common methods applied to zeolites.⁶ Heat treatment involves heating the zeolite to high temperatures, which facilitates the dehydration of adjacent silanol groups, leading to the formation of robust Si–O–Si bridges.⁷ This process effectively condenses adjacent silanol defects, thereby strengthening the zeolite framework and improving its thermal stability. However, this treatment

is not effective for isolated silanol groups that lack neighboring silanol groups for further condensation, limiting the potential for extreme stability. The second common method is the steam treatment which is widely used in the industry for defect healing and dealumination processes.⁵ During steam treatment, high-temperature conditions can lead to the extraction of framework aluminum species, resulting in the formation of T-site vacancies in the zeolite structure. However, these vacancies are not permanent and can be partially healed as silicate species migrate from other regions within the zeolite framework to fill the voids.^{8,9} This migration process, demonstrated in prior studies, underscores the potential of steam treatment to minimize silanol defects and restore structural integrity. Optimizing the steam treatment conditions, such as the temperature, duration, and amount of water introduced, can therefore maximize the defect-healing effects, particularly under the harsh conditions that zeolites often face in practical applications.

Here, the aim is to optimize the thermal stability of high silica FAU zeolites, a class of large-pore zeolites with exceptional performance in catalysis and separation.^{5,10,11} FAU zeolites are widely regarded as some of the most industrially significant zeolites, but their use in extreme environments, such as those exceeding 1000 °C, demands appropriate approaches to enhance their structural stability.^{5,12,13} To address this, we selected a commercial FAU zeolite with the highest available Si/Al ratio and systematically subjected it to various treatment conditions, including different temperatures, durations, and water contents. This study reveals that steam treatment with trace amounts of water is particularly effective in enhancing the thermal stability of FAU zeolites. The optimal sample, treated at 650 °C for 24 hours with the existence of 1% water vapor, retained 69% of its relative crystallinity relative to the as-purchased FAU after a 24-hour heat resistance test at 1150 °C. The reduction in relative crystallinity was halved compared to the untreated sample under the same conditions, indicating significantly improved thermal stability. In comparison, dry heat treatment under identical conditions yielded lower thermal stability, with crystallinity retention at 63%.

^a Department of Chemical System Engineering, The University of Tokyo, 7-3-1 Hongo, Bunkyo-ku, Tokyo 113-8656, Japan.

E-mail: wakihara@chemsys.t.u-tokyo.ac.jp

^b Department of Environment Systems, Graduate School of Frontier Sciences, The University of Tokyo, 5-1-5 Kashiwanoha, Kashiwa-shi, Chiba 277-8563, Japan

^c Precursory Research for Embryonic Science and Technology, Japan Science and Technology Agency, Kawaguchi, Saitama 332-0012, Japan

^d Institute of Engineering Innovation, The University of Tokyo, 2-11-16 Yayoi, Bunkyo-ku, Tokyo 113-8656, Japan

^e Graduate School of Engineering, Chiba University, 1-33 Yayoi-cho, Inage-ku, Chiba 263-8522, Japan

† Electronic supplementary information (ESI) available. See DOI: <https://doi.org/10.1039/d5cc00510h>



A commercial FAU zeolite with the highest Si/Al ratio available (Tosoh, HSZ-390HUA, Si/Al ratio 385) was selected for the treatments. This choice was intentional to further enhance the intrinsic thermal stability of FAU, aiming to develop an extremely stable FAU zeolite capable of withstanding harsh conditions. Moreover, the high Si/Al ratio minimizes complications arising from dealumination during steam treatment, a common phenomenon that can occur in zeolites with high aluminium content. Dealumination alters the framework structure, complicating the analysis of treatment effects. The commercial FAU zeolite was labelled as FAU-as-purchased and subjected to treatments in a custom-built apparatus (Fig. S1, ESI[†]),⁵ where samples were heated to a target temperature (T) after a 75-minute ramp-up and held for several hours (t). A specific volume of water was introduced *via* a syringe pump, mixed with high purity dry air to generate x vol% steam at atmospheric pressure. As a result, samples were labelled as FAU- $T(^{\circ}\text{C})$ - $x(\%)$ - $t(\text{h})$. The relative crystallinity of each sample in this study was evaluated using powder X-ray diffraction (XRD), focusing on peaks in the 2θ range of 20° to 30° through deconvolution and integration techniques. In addition, all the relative crystallinity values reported here are relative to the FAU-as-purchased.

The relative crystallinities of all treated samples are summarized in Table S1 (ESI[†]). All samples retained relative crystallinities of $\geq 94\%$, indicating that the FAU framework is robust enough to withstand the treatments. The morphology of the samples before and after treatments was assessed by SEM. The FAU-as-purchased zeolite, depicted in Fig. S2 (ESI[†]), exhibits an agglomerated morphology with crystals showing a uniform size distribution ranging from 100 nm to 300 nm. After the treatments, SEM images reveal no observable morphological changes among all treated samples with some representative images presented in Fig. S2 (ESI[†]), confirming that the treatments do not affect the crystal size or morphology of FAU. These results demonstrate that both steam and heat treatments preserve the structural integrity and morphology of the FAU zeolite.

Fig. S3 (ESI[†]) presents the ^{29}Si MAS NMR spectra of FAU-as-purchased and representative treated samples. The single-pulse spectra reveal a dominant resonance at -106.5 ppm, attributed to Q^4 $[\text{Si}-(\text{OSi})_4]$ silicon species. The absence of Q^3 $[(\text{HO})-\text{Si}-(\text{OSi})_3]$ signals indicates that no detectable silanol defects are present in any of the samples.¹⁴ Furthermore, the ^{29}Si CP MAS NMR spectra lack any detectable signals, providing additional evidence that all samples are free of silanol nests. The minimal differences between the as-purchased and treated samples suggest that the as-purchased FAU is of high quality and free of silanol nests. To further investigate silanol groups in FAU before and after the treatment, FT-IR spectroscopy was employed. The normalized FT-IR spectra of FAU samples shown in Fig. 1(a) present an absorption band at 3750 – 3720 cm^{-1} , corresponding to isolated silanol groups $[(\text{HO})-\text{Si}-(\text{OSi})_3]$.⁶ A decrease in intensity of this band is observed for the treated samples compared to the FAU-as-purchased. Among the treated samples, FAU- 650°C - 1% - 24 h shows the lowest intensity, indicating the most significant reduction in isolated silanol groups. Additionally, the absence of a broad absorption band between 3650 – 3500 cm^{-1} in all spectra further confirms the lack of hydrogen-bonded silanol groups, commonly referred to as

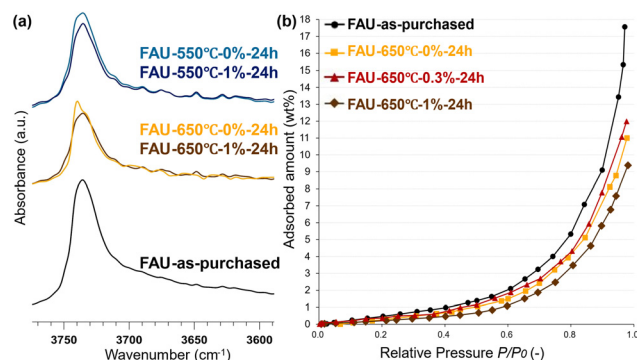


Fig. 1 Normalized FT-IR spectra (a) and water vapor adsorption isotherms (b) of as-purchased and representative treated FAU samples.

silanol nests. It has been shown that in high-silica zeolites, the quantity of silanol groups play an important role in determining the hydrophobicity of the framework.¹⁵ To assess the impact of treatments on the hydrophobicity of FAU, water vapor adsorption was measured at 25°C . The adsorption isotherms of the FAU-as-purchased and after representative treatments are shown in Fig. 1(b). The untreated FAU sample exhibits a water adsorption capacity at $P/P_0 = 0.8$ of $5.3\text{ wt}\%$, while the treated samples show reduced capacities, around $4\text{ wt}\%$, highlighting the enhanced hydrophobicity achieved through treatment. Among the treated samples, FAU- 650°C - 1% - 24 h demonstrates the lowest water adsorption capacity of $3.5\text{ wt}\%$ ($P/P_0 = 0.8$), slightly outperforming the other two treated samples. This result aligns with the FT-IR findings, confirming that the trace water-assisted steam treatment is highly effective in reducing isolated silanol groups. The pronounced reduction in both isolated silanol groups and water adsorption capacity for FAU- 650°C - 1% - 24 h suggests that the trace water-assisted steam treatment may induce silicate migration.^{8,9,16} This process likely enhances the removal of silanol defects, underscoring the superior effectiveness of this treatment in defect minimization and hydrophobicity enhancement.

To assess the thermal stability of all samples before and after the treatment, heat resistance tests were conducted at 1150°C . The temperature ramped up over 4 h and was maintained for 20 h . After the tests, the non-treated FAU sample was named as FAU-as-purchased-tested, while the treated samples were denoted as FAU- $T(^{\circ}\text{C})$ - $x(\%)$ - $t(\text{h})$ -tested. Fig. 2(a) displays powder XRD patterns of samples treated under various conditions (e.g., water content of 0 – 1% and treatment duration of 24 h) after heat resistance tests, with the relative crystallinity of all samples summarized in Table 1. The FAU-as-purchased-tested sample retained a relative crystallinity of 34% after exposure to extreme conditions (1150°C for 24 h). While this value is relatively high given the severity of the thermal treatment, it highlights the necessity for further stabilization to achieve the exceptional thermal stability required for demanding applications. The treated samples exhibited significant improvements in thermal stability. Among them, FAU- 650°C - 1% - 24 h -tested exhibited a remarkable relative crystallinity of 69% , demonstrating a substantial improvement in thermal stability compared to the FAU-as-purchased-tested sample. This significant enhancement underscores the effectiveness of carefully optimized



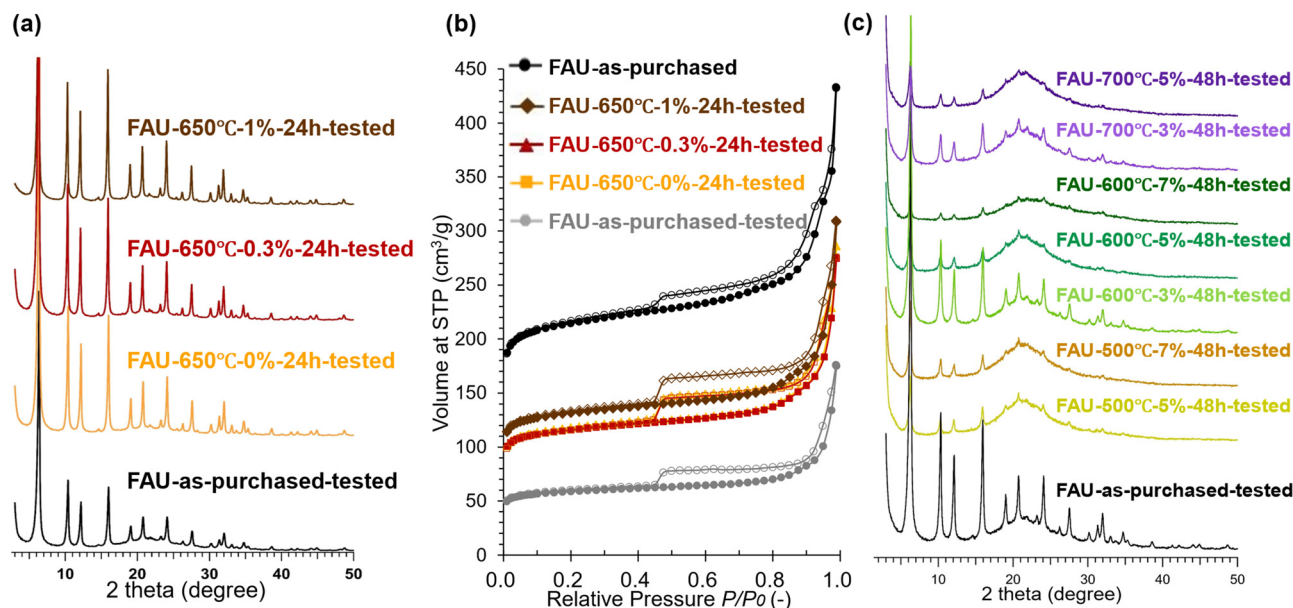


Fig. 2 (a) Powder XRD patterns of representative heat/steam treated FAU samples after performing the heat resistance test at 1150 °C for 24 h; (b) nitrogen adsorption–desorption isotherms of FAU samples. Solid symbols refer to adsorption and open symbols represent desorption; (c) powder XRD patterns of FAU samples treated under severe steam conditions after performing the heat resistance test at 1150 °C for 24 h.

Table 1 The relative crystallinity of FAU samples, relative to the as-purchased FAU, after a 24-hour heat resistance test at 1150 °C under various treatment conditions

Sample name	Relative crystallinity (%)
FAU-as-purchased-tested	34
FAU-700 °C-1%-24 h-tested	63
FAU-650 °C-2%-24 h-tested	66
FAU-650 °C-1%-48 h-tested	65
FAU-650 °C-1%-24 h-tested	69
FAU-650 °C-1%-12 h-tested	62
FAU-650 °C-0.3%-24 h-tested	63
FAU-650 °C-0%-24 h-tested	63
FAU-600 °C-1%-24 h-tested	65
FAU-600 °C-0.3%-24 h-tested	61
FAU-600 °C-0%-24 h-tested	60
FAU-550 °C-1%-24 h-tested	61
FAU-550 °C-0.3%-24 h-tested	59
FAU-550 °C-0%-24 h-tested	56

steam/heat treatments. These treatment conditions, particularly with trace water content, played a critical role in stabilizing the framework and enhancing thermal stability. Further examination of the treated samples revealed that trace amounts of water during steam treatment played a vital role in determining the effectiveness of the treatment. Samples treated with 1% water content consistently outperformed those treated in either dry air or higher humidity conditions. For instance, FAU-650 °C-0%-24 h-tested had a relative crystallinity of 63%, compared to the 69% observed for FAU-650 °C-1%-24 h-tested. Fig. 2(b) depicts the nitrogen adsorption–desorption isotherms of FAU-as-purchased and samples after heat resistance tests. Analysis of the isotherms reveals a hysteresis loop at relative pressures of $P/P_0 \approx 0.5$, indicating the presence of mesopores and intraparticle voids. Surface area and micropore volumes, calculated using the BET and t -plot methods respectively,

are summarized in Table S2 (ESI[†]). Significant reductions in both surface area and micropore volume were observed in samples after the heat resistance tests, which align with the decrease in relative crystallinity. These findings suggest partial amorphization of the zeolite frameworks. Among all tested samples, FAU-650 °C-1%-24 h-tested maintained the highest surface area and micropore volume, further confirming its enhanced framework stability and optimized treatment conditions.

Heat stability tests were also performed in FAU zeolites treated under relatively severe treatment conditions to confirm the steam concentration effect in the stabilization of the framework. Fig. 2(c) illustrates the powder XRD patterns of samples treated under relatively higher water content of 3–7% and treatment duration of 48 hours after the heat resistance test. The relative crystallinity of all treated samples decreased significantly compared to the as-purchased FAU, indicating a reduction in framework stability caused by harsh steam treatment. Also, increased humidity during treatment proved detrimental. This trend is particularly pronounced when examining the three samples treated at 600 °C. This highlights the adverse effects of excessive water content during treatment on the thermal stability of the FAU framework. These observations indicate that both steam treatment with excessive humidity and completely dry heat treatment yield less favorable results. The samples treated with trace water-assisted steam treatment consistently exhibited superior performance compared to others. This improvement is potentially due to the role of trace water in facilitating silicate migration, which promotes the condensation of isolated silanol groups and consequently enhances the structural integrity and thermal stability of the zeolite framework.

These results demonstrate that optimized steam/heat treatment conditions, such as those employed for FAU-650 °C-1%-24



h-tested, achieve a balance between sufficient water to promote silicate migration and minimal water to prevent compromise of the framework. Reduced isolated silanol absorption bands in FT-IR spectra and lower water vapor adsorption capacity further supports the enhanced stabilization. These findings underscore the critical role of trace water in improving the thermal stability of high-silica FAU zeolites.

In conclusion, this study investigates the impact of various treatment conditions on the thermal stability of high-silica FAU zeolites. By using a high-silica FAU zeolite, we focused exclusively on the role of silanol defect healing, shedding light on how manipulating silanols can improve the stability of the framework. Steam/heat treatments significantly improved thermal performance, with steam treatment at high temperature and trace water content proving particularly effective. This approach reduced isolated silanol groups, increased hydrophobicity, and enhanced thermal stability. The optimized treatment (1% humidity, 650 °C, 24 h) significantly improved thermal stability, reducing the loss of relative crystallinity after the 1150 °C, 24-hour heat resistance test by more than half compared to the untreated sample. These findings underscore the crucial role of water in defect healing, as steam treatment not only promotes silanol condensation but may also facilitate the migration of silicate species within the framework, further reinforcing stability. This study presents a feasible approach to achieving ultra-high thermal stability in zeolites through post-synthetic treatments and underscores three key insights: (1) the fundamental role of water in steam-assisted defect healing, (2) the significant influence of silanol defects on zeolite stability, and (3) the potential for optimizing treatment conditions to enhance material performance.

Boqing Li: investigation, methodology, data curation, writing – original draft. Takahiro Ohkubo: ²⁹Si MAS NMR data curation. Toru Wakihara: supervision, project Administration. All authors: writing – review & editing.

This research received support from the New Energy and Industrial Technology Development Organization (NEDO) Moonshot Research, JSPS KAKENHI the Grant-in-Aid for Scientific Research (S) (JP21H05011 and JP23H05454) and the Grants-in-Aid for Transformative Research Areas (A) (JP20A206/20H05880), and Ministry of Education, Culture, Sports, Science and Technology

(MEXT) “Establish Process Science toward Commercialization of Materials (Materialize)” Project (JPMXP0219192801).

Data availability

The data supporting this article have been included as part of the ESI.†

Conflicts of interest

There are no conflicts to declare.

Notes and references

- 1 R. Simancas, A. Chokkalingam, S. P. Elangovan, Z. Liu, T. Sano, K. Iyoki, T. Wakihara and T. Okubo, *RSC*, 2021, 12, 7677–7695.
- 2 L. Zhang, K. Chen, B. Chen, J. L. White and D. E. Resasco, *J. Am. Chem. Soc.*, 2015, 137, 11810–11819.
- 3 S. Proding, H. Shi, S. Eckstein, J. Z. Hu, M. V. Olarte, D. M. Camaioni, M. A. Derewinski and J. A. Lercher, *Chem. Mater.*, 2017, 29, 7255–7262.
- 4 K. Iyoki, K. Kikumasa, T. Onishi, Y. Yonezawa, A. Chokkalingam, Y. Yanaba, T. Matsumoto, R. Osuga, S. P. Elangovan, J. N. Kondo, A. Endo, T. Okubo and T. Wakihara, *J. Am. Chem. Soc.*, 2020, 142, 3931–3938.
- 5 K. Iyoki, Y. Yamaguchi, A. Endo, Y. Yonezawa, T. Umeda, H. Yamada, Y. Yanaba, T. Yoshikawa, K. Ohara, K. Yoshida, Y. Sasaki, T. Okubo and T. Wakihara, *Microporous Mesoporous Mater.*, 2018, 268, 77–83.
- 6 I. C. Medeiros-Costa, E. Dib, N. Nesterenko, J. P. Dath, J. P. Gilson and S. Mintova, *RSC*, 2021, 50, 11156–11179.
- 7 I. Grosskreuz, H. Gies and B. Marler, *Microporous Mesoporous Mater.*, 2020, 291, 09683.
- 8 M. Sasaki, Y. Sato, Y. Tsuboi, S. Inagaki and Y. Kubota, *ACS Catal.*, 2014, 4, 2653–2657.
- 9 T. Ikeda, S. Inagaki, T. A. Hanaoka and Y. Kubota, *J. Phys. Chem. C*, 2010, 114, 19641–19648.
- 10 Y. Sada, S. Miyagi, K. Iyoki, M. Yoshioka, T. Ishikawa, Y. Naraki, T. Sano, T. Okubo and T. Wakihara, *Microporous Mesoporous Mater.*, 2022, 334, 112196.
- 11 Q. Wang, H. Chen, F. He, Q. Liu, N. Xu, L. Fan, C. Wang, L. Zhang and R. Zhou, *Membranes*, 2023, 13, 13110858.
- 12 R. M. Heck and R. J. Farrauto, *Automob. Exhaust Catal.*, 2001, 221, 443–457.
- 13 H. S. Cerqueira, G. Caeiro, L. Costa and F. Ramôa Ribeiro, *J. Mol. Catal. A:Chem.*, 2008, 292, 1–13.
- 14 Q. Yu, W. Zhang, J. Li, W. Liu, Y. Wang, W. Chu, X. Zhang, L. Xu, X. Zhu and X. Li, *Microporous Mesoporous Mater.*, 2023, 13, 112570.
- 15 B. Li, K. Iyoki, P. Techasarintr, S. P. Elangovan, R. Simancas, T. Okubo, T. Yokoi and T. Wakihara, *ACS Catal.*, 2023, 13, 15155–15163.
- 16 L. H. Ong, M. Dömök, R. Olindo, A. C. Van Veen and J. A. Lercher, *Microporous Mesoporous Mater.*, 2012, 164, 9–20.

